Ultrasound-Enhanced siRNA Delivery Using Magnetic Nanoparticle-Loaded Chitosan-Deoxycholic Acid Nanodroplets

*Jeong Yu Lee, Calum Crake, Boon Teo, Dario Carugo, Marie de Saint Victor, Anjali Seth, and Eleanor Stride**

Small interfering RNA (siRNA) has significant therapeutic potential but its clinical translation has been severely inhibited by a lack of effective delivery strategies. Previous work has demonstrated that perfluorocarbon nanodroplets loaded with magnetic nanoparticles can facilitate the intracellular delivery of a conventional chemotherapeutic drug. The aim of this study is to determine whether a similar agent can provide a means of delivering siRNA, enabling efficient transfection without degradation of the molecule. Chitosan-deoxycholic acid nanoparticles containing perfluoropentane and iron oxide (d_0 = 7.5 ± 0.35 nm) with a mean hydrodynamic diameter of 257.6 ± 10.9 nm are produced. siRNA (AllStars Hs cell death siRNA) is electrostatically bound to the particle surface and delivery to lung cancer cells and breast cancer cells is investigated with and without ultrasound exposure (500 kHz, 1 MPa peak-to-peak focal pressure, 40 cycles per burst, 1 kHz pulse repetition frequency, 10 s duration). The results show that siRNA functionality is not impaired by the treatment protocol and that the nanodroplets are able to successfully promote siRNA uptake, leading to significant apoptosis (52.4%) 72 h after ultrasound treatment.

1. Introduction

The ability of small interfering RNA (siRNA) to block the translation of messenger RNA encoding aberrant disease-associated proteins in a powerful and selective manner provides it with huge therapeutic potential. Across a wide range of pathologies siRNA offers a means of specifically knocking down the expression of the disease causative factor. A prime example of its possible utility is in the treatment of cancer where degradation of mRNA encoding antiapoptotic proteins may even enable a synergistic increase in the efficacy of conventional chemotherapeutic agents.[1] To date, however, the potential of siRNA has not been realized clinically due to its inefficient systemic delivery. Notably, in its naked form, siRNA suffers from poor pharmacokinetics due to its low bloodstream stability and rapid glomerular filtration. Furthermore, target cell transfection efficiency is very low because it has no intrinsic mechanism for cell entry. In vitro this limitation can be overcome with the use of positively charged polymer-based delivery vectors, but in vivo these vectors are too unstable and the electrostatic mediated cell entry mechanism upon which they rely is too unspecific.[2] While liposomal delivery systems can provide enhanced circulation time thus benefiting from the enhanced permeability and retention effect, they achieve very limited penetration beyond the perivascular space of the tumor and do not efficiently release their cargo.[3]

There have been a number of recent studies demonstrating the potential of ultrasound as a means of promoting siRNA delivery both in vitro and in vivo.[4,5] Ultrasound mediated delivery can be significantly enhanced through the use of gas microbubbles that provide a means of encapsulating and improving tissue penetration and uptake of various therapeutics, including siRNA. For example, Carson et al. used microbubbles for inhibition of endothelial growth factor (EGF) receptor signaling, an established strategy for treating numerous types of cancer. Their results indicated that tumor growth could be decelerated, arrested or even reversed in EGFR-treated mice.[4] Florinas et al. similarly showed that microbubbles loaded with PEI (polyethylamine) encapsulating siRNA could induce knockdown of vascular EGF in vitro and decelerate tumor growth in vivo in a mouse model.[6] A further advantage of this approach is that the timescales for treatment are significantly reduced compared to passive delivery methods. Typically, ultrasound is applied within minutes following injection. Thus the risk of

Dr. J. Y. Lee, Dr. C. Crake, Dr. B. Teo, Dr. D. Carugo, Dr. M. de Saint Victor, Dr. A. Seth, Prof. E. Stride
Institute of Biomedical Engineering
Department of Engineering Science
University of Oxford
Oxford, Old Road, Campus OX3 7DQ, UK
E-mail: eleanor.stride@eng.ox.ac.uk
Dr. D. Carugo
Faculty of Engineering and the Environment
Southampton University
Southampton SO17 1BJ, UK

DOI: 10.1002/adhm.201601246

Table 1. Formulations of nanodroplets and nanoparticles used in the experiments.

	Nanodroplets/Materials	CND	CND/siRNA	CND/neg	CP	CP/siRNA
Core	Magnetic nanoparticles (C_{Fe}, mmol)	48	48	48	48	48
	Perfluoropentane (PFP, μL)	10	10	10	0	0
Shell	Chitosan-Deoxycholic acid conjugates (mg)	5	5	5	5	5
	siRNA phenotype	0	Cell death	Green Fluorescent Protein	0	Cell death

siRNA degradation due to prolonged exposure to the in vivo environment is reduced.

Microbubbles however have a number of disadvantages as delivery agents: they are physically confined to the vasculature and have comparatively poor circulatory stability, typically exhibiting half-lives of a few minutes.[7] In order to address these challenges, volatile liquid nanodroplets have been widely investigated over the past 5–10 years as an alternative means of promoting ultrasound mediated delivery. Upon exposure to ultrasound the liquid droplets undergo a phase transition to form gas microbubbles, but their initial nanoscale size enables them to both remain in circulation for much longer periods of time and to extravasate.[8] We have previously demonstrated that both the stability and phase conversion efficiency of nanodroplets can be considerably improved by the inclusion of iron oxide nanoparticles.[9] The resulting droplets were able to enhance the delivery of a conventional chemotherapy drug, paclitaxel, generating a 40% improvement in cytotoxicity compared with free drug.

One potential drawback of liquid nanodroplets, however, is that the phase transition process is associated with large volume changes and more energetic microbubble activity than that produced by preformed gas bubbles.[10] Thus there is a potential risk of collateral damage to the surrounding tissues and also to the therapeutic material. This is particularly problematic with molecules such as siRNA that are easily degraded.[11] The aim of this study therefore was to investigate whether particle stabilized liquid nanodroplets could be used for delivery of siRNA without impairing functionality.

2. Results and Discussion

2.1. Particle Characteristics

The nanodroplet and nanoparticle formulations used in the experiments are summarized in **Table 1**. The mean hydrodynamic diameter of the chitosan-deoxycholic acid coated perfluoropentane nanodroplets (CNDs) (**Figure 1**a) in deionized water was 257.6 ± 10.9 nm as determined by dynamic light scattering at 37 °C (Figure 1b). This increased to 3822.2 ± 226.4 nm when the suspension was exposed to ultrasound (1.8 MHz and 335 kPa peak negative pressure) for 45 s continuously, indicating that the encapsulated perfluoropentane (PFP) underwent a phase change from liquid to gas. The average diameter of the chitosan-deoxycholic acid solid particles (CPs) was 170.6 ± 8.9 nm and this changed only slightly to 181.7 nm upon ultrasound exposure (Figure S5, Supporting Information). The zeta potential of the CNDs decreased from +57.4 to +40.7 mV following ultrasound exposure (Figure 1c), corresponding to a decrease of 29.1% in the surface charge density (please note that the increase in the surface area of the droplets was much larger, by an average factor of 219.5). This may be beneficial in facilitating intracellular uptake of siRNA by decreased electrostatic force after ultrasound treatment.

Figure 1d shows transmission electron microscopy (TEM) images of CND before and after ultrasound exposure (see also Figures S2 and S3, Supporting Information). In the left-hand image, white spots are clearly visible corresponding to PFP surrounded by darker rings indicating uranyl acetate stained chitosan-deoxycholic acid shells.[12] Following ultrasound exposure however, these were no longer visible and were replaced with irregularly shaped particles that were likely produced by fragmentation of the shell during droplet expansion. There is an apparent discrepancy between the size of some of the droplets shown in Figure 1d,c prior to ultrasound exposure. This is likely to be due to vaporization of a portion of the droplets having occurred in the vacuum environment of the TEM. The bubbles formed during ultrasound exposure were only stable when suspended in a 10% glycerol solution (Figure 1c) and so are not visible in the post ultrasound TEM image. There are some very small white spots visible in the right-hand panel of Figure 1d and in Figure S3 (Supporting Information), which may be droplets that did not vaporize. This is not unexpected since droplets with diameters of ≈100 nm, will have a much higher vaporization temperature than particles of 200 nm[12] and correspondingly the acoustic pressure required to produce expansion (i.e., the cavitation threshold or Blake pressure[13]) will also be higher.

2.2. Ultrasound Response

Figure 2a, shows bright field optical microscope images of CNDs captured before and after 45 s of continuous wave (CW) ultrasound exposure (1.8 MHz and 335 kPa peak negative pressure). Conversion of nanodroplets to microbubbles was readily observed over this time period. The theoretical size of the microbubbles, calculated using the ideal gas law, was 2.3 μm at 37 °C, whereas the experimentally measured average diameter was equal to 6.3 μm.[14] However, the theoretical prediction did not take into account the additional surface pressure produced by the shell, coalescence of individual bubbles in close proximity to each other, or absorption of dissolved gases from the phosphate buffered saline (PBS).[9,15] Moreover, there may have been an effect of temperature rise over the course of the experiment, although the maximum liquid temperature measured after 3 min of continuous wave ultrasound exposure was only ≈42 °C (Figure S6, Supporting Information).

In order to detect any changes in the chitosan-deoxycholic acid shell, CND loaded with Nile red dye were also observed in the

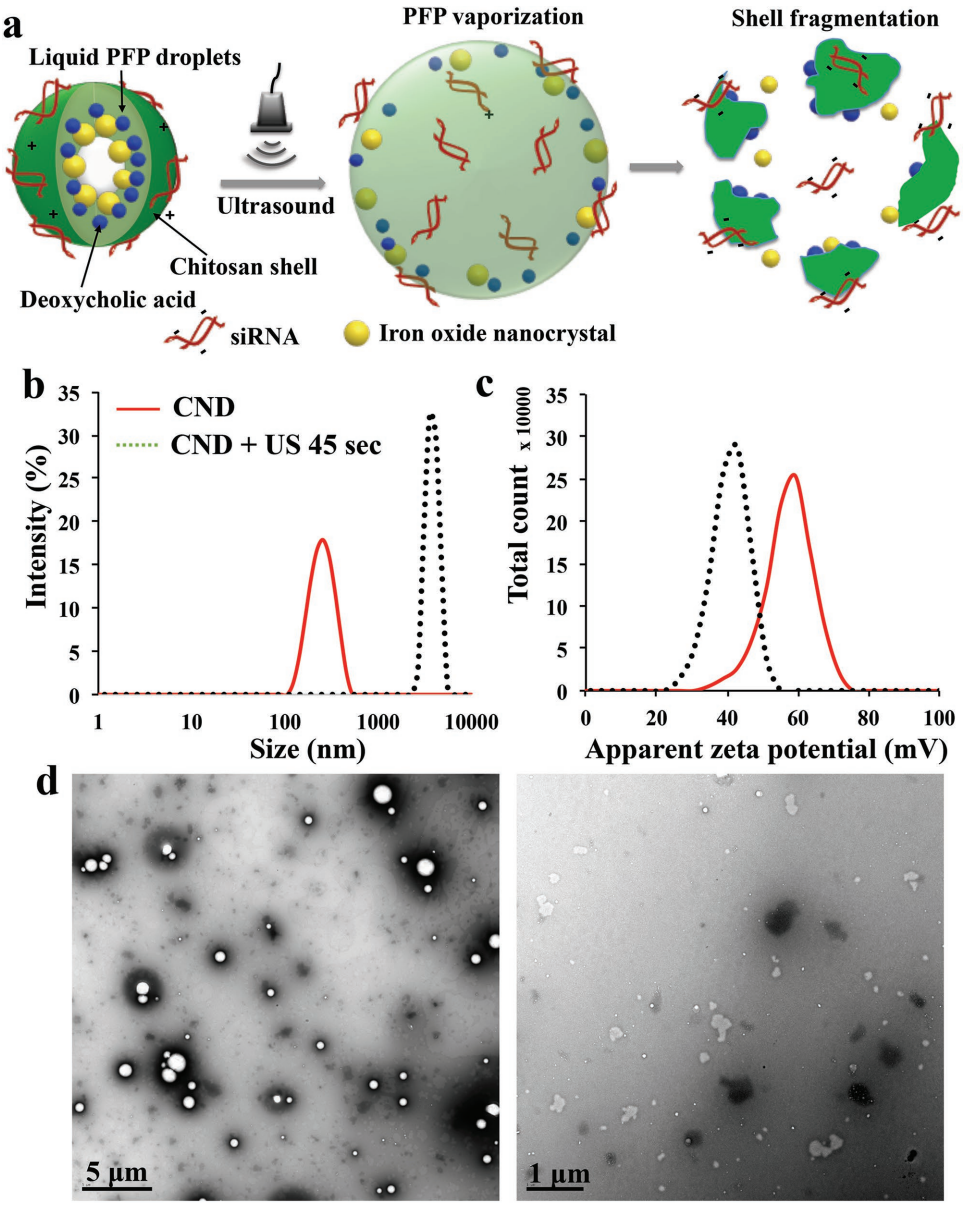

Figure 1. a) Schematic representation of chitosan-deoxycholic acid coated perfluoropentane nanodroplets (CNDs). b) Hydrodynamic diameters of CNDs before (solid line) and after (dotted line) exposure to ultrasound for 45 s in 10% glycerol in water. c) Zeta potential of CNDs before and after ultrasound exposure. d) TEM images of CND before (left) and after (right) ultrasound exposure for 45 s.

same system under a fluorescent microscope (Figure 2b). Nile red is lipophilic and so would be expected to label the strongly hydrophobic deoxycholic acid. Before ultrasound exposure, a collection of small fluorescent objects were visible. After ultrasound exposure, larger spherical objects with fluorescent coating could be clearly observed, indicating the formation of coated microbubbles.

Changes in the concentration of CND between 100 and 1000 nm for different ultrasound exposure times were measured using a Nanosight system. The concentration of CND decreased from to 8.99×10^8 to 5.80×10^8 particles mL^{-1} after 60 s of CW exposure. This reduction indicates that 45% of CND responded to ultrasound in 1 min, and 57% in 2 min and then moved out of the measuring range. By contrast, the change in CP concentration showed an increase of ≈23% at longer exposure times. This may have been due to the breakup of CP clusters: the size distribution of CPs also changed after ultrasound exposure with broadening of the main peak and the appearance of a second peak at ≈15 nm (Figure S5, Supporting Information).

2.3. Magnetic Response

As mentioned above, magnetic particles were incorporated into the droplets to improve vaporization efficiency. They can also facilitate droplet localization for targeted delivery. Magnetic retention of CND was observed in a 127 µm × 50 µm microfluidic channel into the substrate of which were embedded a small permanent magnet and an ultrasound transducer.[16] As shown in

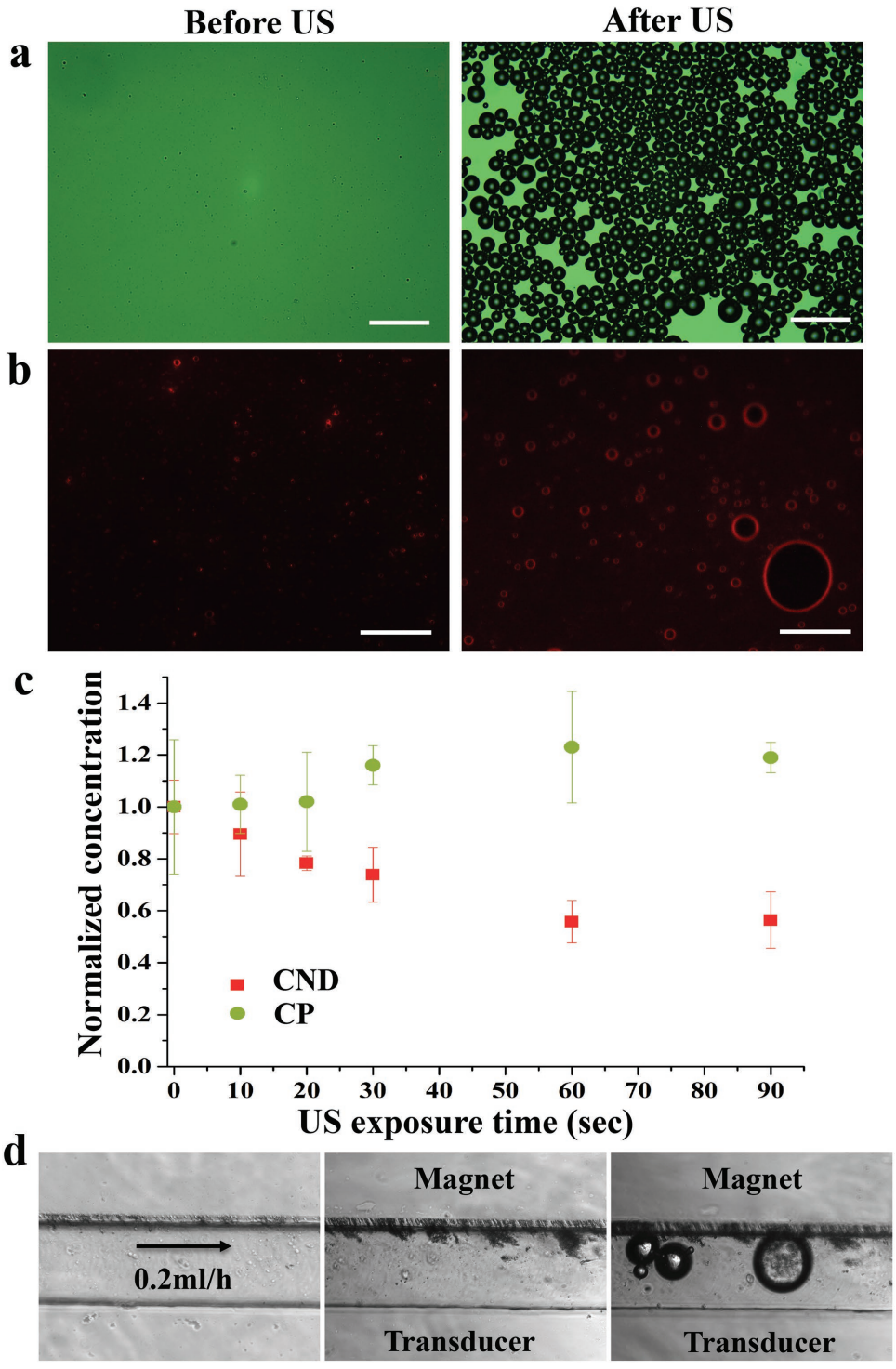

Figure 2. a) Optical microscope images of CNDs before and after ultrasound exposure for 45 s. Scale bars indicate 200 µm. b) Fluorescent images of Nile red-loaded CNDs before and after ultrasound exposure for 45 s. Scale bars indicate 200 µm. c) Normalized concentration changes of CNDs and CPs upon different ultrasound exposure times. d) Accumulation of CNDs at the target site under the influence of a magnetic field and vaporization by ultrasound exposure. The CNDs were dispersed in PBS, and the flow rate was 0.2 mL h^{-1}. After 2 min of flow, ultrasound was applied from the opposite side of the channel.

the microscope images reported in Figure 2d, at a fixed flow rate of 2 mL h^{-1}, CNDs were concentrated at the wall of the channel closest to the magnet. After 2 min, ultrasound was applied from the opposite side of the channel. Microbubbles were continuously generated from the accumulated droplets and retained in the region by the magnet. These observations also confirmed

successful incorporation of the iron oxide nanoparticles, whose size (7.5 nm) was too small to be detected using the available microscopy facilities.

2.4. siRNA Viability

One concern associated with ultrasound mediated delivery is the potential for damaging therapeutic molecules. The impact of ultrasound on the Naked AllStar siRNA and randomly scrambled siRNA was therefore investigated at different ultrasound exposure times (0, 10, 30, 60, and 120 s). Following exposure, an agarose gel retardation assay was used to detect any siRNA degradation or structural change (**Figure 3**a). Electrophoretic mobility of siRNA in agarose gel was observed, and clear bands appeared at a same row for all siRNA without drag marks, which indicated that siRNA did not undergo any significant degradation under the action of continuous wave ultrasound.

In order to determine whether ultrasound exposure had any effect upon the gene silencing efficiency of siRNA, the viability of A549 cells exposed to lipofectamine-siRNA complexes and ultrasound was compared using the MTS cell proliferation colorimetric assay. Green fluorescent protein (GFP) siRNA was used as a negative control for these experiments. After 48 and 72 h incubation, cells treated with the GFP siRNA formulation showed no significant change in viability (Figure 3b). Conversely, all samples treated with AllStar siRNA underwent a reduction in cell viability that was more pronounced at 72 h compared to 48 h, indicating successful gene knockdown. The ultrasound exposure time had no effect upon the observed changes in viability.

2.5. siRNA:CND Ratio Optimization

To determine the most effective ratio of AllStar siRNA to CND, gel electrophoresis was conducted with CND-siRNA complexes containing different weight ratios of CND to siRNA (Figure 3c). At a weight ratio of 48, the complexes showed retarded migration in the gel. Samples were also examined after ultrasound exposure to assess whether siRNA detachment had occurred. After 15 min of gel retardation, there was no significant migration beyond the loading holes, which indicated that either CND did not release siRNA or it quickly reattached. This is likely to be beneficial for systemic delivery of siRNA. First, attachment to a carrier has been shown to stabilize siRNA in the circulation.[17] Second, siRNA does not readily cross cell membranes through passive diffusion but if it remains attached to fragments of the CND shell this may promote formation of stable endocytotic vesicles.[18] In addition, if the CND is in sufficiently close proximity to the target cell then contact area will be greatly increased during phase transition.

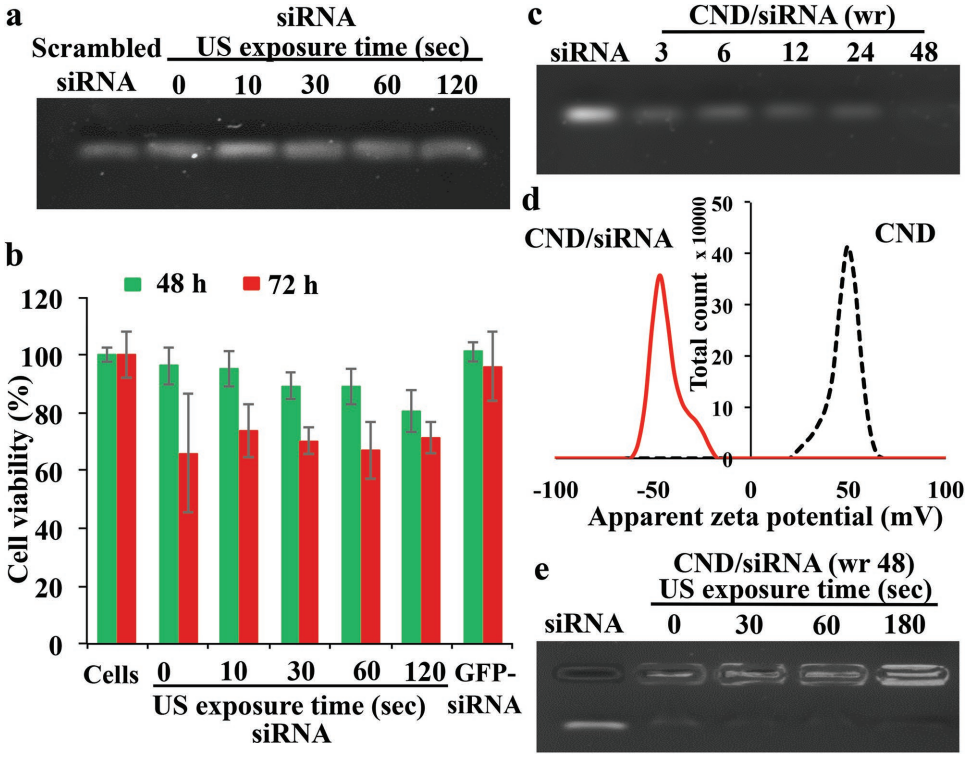

Figure 3. a) Gel retardation assay of scrambled siRNA and AllStar siRNA exposed to ultrasound at increasing exposure times (0, 10, 30, 60, 120 s). b) The viability of A549 cells treated with AllStar siRNA-lipofectamine complexes or GFP siRNA-lipofectamine complexes and then incubated for 48 h (green) and 72 h (red). Prior to treatment, AllStar siRNA was exposed to ultrasound for 0, 10, 30, 60, and 120 s and then complexed with lipofectamine. c) Complexation test of CND and siRNA in water. Each CND-siRNA complex was prepared at a weight ratio (wr) of CND to siRNA from 0 to 48. d) Zeta potential values of CND (dashed line) and CND-siRNA (solid line) in water. e) Gel retardation assay of CND-siRNA decomplexation induced by exposure to ultrasound for different times.

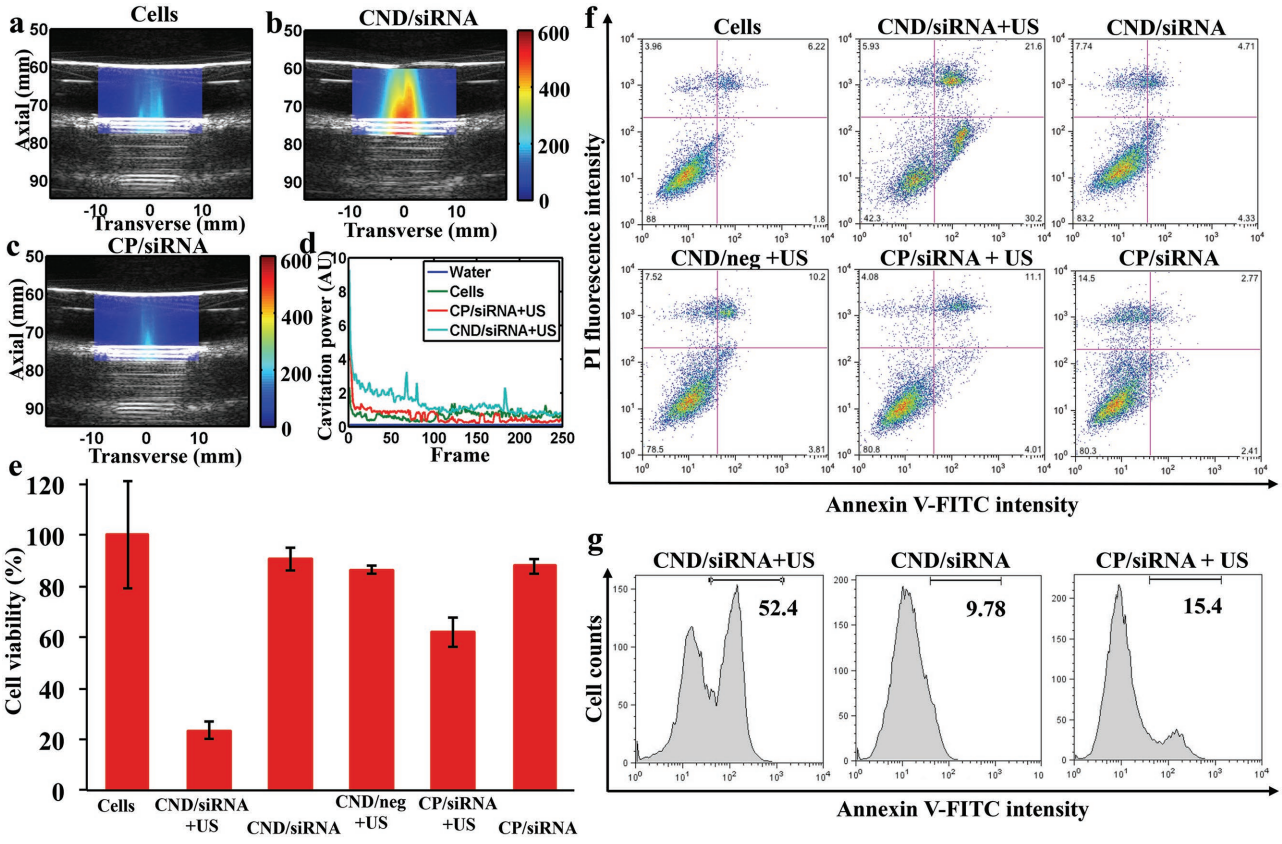

Figure 4. Pre-exposure B-mode images with PAM overlay showing sum of all frames for each exposure, a) for cells only, b) CND/siRNA, and c) CP/siRNA. Color bars represent cavitation energy (AU). d) Maximum cavitation power (AU) from each frame of PAM data. e) The viability of cells exposed to ultrasound and incubated for 72 h following treatment with medium, CND/siRNA, CND/negative siRNA, and CP/siRNA shown at an equivalent siRNA concentration of 20×10^{-9} M. f) In vitro assessment of apoptosis in A549 cells incubated for 72 h following treatment. Flow cytometry analysis via annexin V-FITC/PI staining was used to observe the induction of apoptosis. Cells in the lower right quadrant are Annexin-positive cells indicating early apoptotic cells. The cells in the upper right quadrant indicate annexin-positive/PI-positive, late apoptotic cells. g) Annexin V-FITC analysis for CND/siRNA with ultrasound, CND/siRNA, and CP/siRNA with ultrasound showing degree of apoptosis.

2.6. siRNA Delivery

To determine the gene silencing effect of CND-siRNA complexes and ultrasound exposure, the degree of A549 proliferation was examined 72 h after treatment. As shown in **Figure 4**a, exposure to the CND-siRNA complexes and ultrasound inhibited the proliferation of cancer cells in a synergistic manner. A significant reduction in cell viability to 23.4% ± 3.2% was observed, compared to only 90.3% ± 4.5% from the CND-siRNA complexes alone and 87% ± 1.47% from CND complexed with scrambled siRNA and ultrasound.

Solid nanoparticles (CPs) with siRNA produced a negligible decrease in cell viability in the absence of ultrasound. In combination with ultrasound exposure, they did produce some reduction in cell viability, potentially as a result of acoustic streaming and/or radiation force pushing the particles directly into cells.[19]

2.7. Acoustic Emissions

During ultrasound exposure, the evolution of microbubbles was monitored using passive acoustic mapping (PAM).[9] Figure 4a–c shows maps of summed cavitation energy overlaid on B-mode images from each experiment. When water was exposed to ultrasound in the absence of any particles, the maximum PAM signal was 79.26 energy units (please see the Experimental Section) and the energy distribution was comparatively uniform. In the absence of any particles but with cells, a small increase in the PAM signal was detected due to cavitation at the surface of the A549 cells (max value 239.72 energy units). There was no significant change observed upon addition of the CP-siRNA complexes. With the CND-siRNA complexes, however, the maximum PAM signal value was approximately doubled (572.01 energy units) indicating that acoustic emissions are well correlated with therapeutic effect in this system.

2.8. Cell Viability

Apoptosis of A549 cells was also measured 72 h following treatment using annexin V-FITC and propidium iodide (PI) staining (Figure 4f). Cell shrinkage, changes in DNA content and changes in the plasma membrane can be observed using flow

cytometry analysis. In early apoptosis, phosphatidyl serine residues, which have a high affinity for annexin V, are expressed on the cell surface, and an apoptotic cell can thus be detected. The results indicate that there were a large number of annexin V-positive cells in the samples exposed to CND-siRNA complexes and ultrasound.

An intense PI signal was observed from the same group. Interestingly the CP-siRNA complexes produced a slight increase in the number of late apoptotic cells under ultrasound exposure. However it was not sufficient to enhance the delivery efficiency of siRNA and produce a sustained therapeutic effect. In Figure 4g, annexin V-positive cell populations were independently evaluated by flow cytometry. The percentage of cells in the second peak of each panel indicates the total percentage of apoptotic cells.[20] This analysis revealed that the CND-siRNA complexes had a significant effect on inducing cancer cell apoptosis (52.4%) in combination with ultrasound exposure.

2.9. Cell Uptake

Confocal scanning laser microscopy was used to observe the cellular uptake of fluorescent siRNA carried by nanodroplets to GFP-expressing MCF7 cells (**Figure 5**). After 5 min of incubation without ultrasound exposure, low intensity red fluorescence was detected in the cells incubated with CND-siRNA complexes. This was significantly increased by ultrasound exposure even with thorough washing after treatment. Furthermore, widespread distribution of red fluorescent siRNA was achieved by ultrasound stimulation. Ultrasound exposure was not found to promote delivery of free siRNA, i.e., in the absence of CNDs.

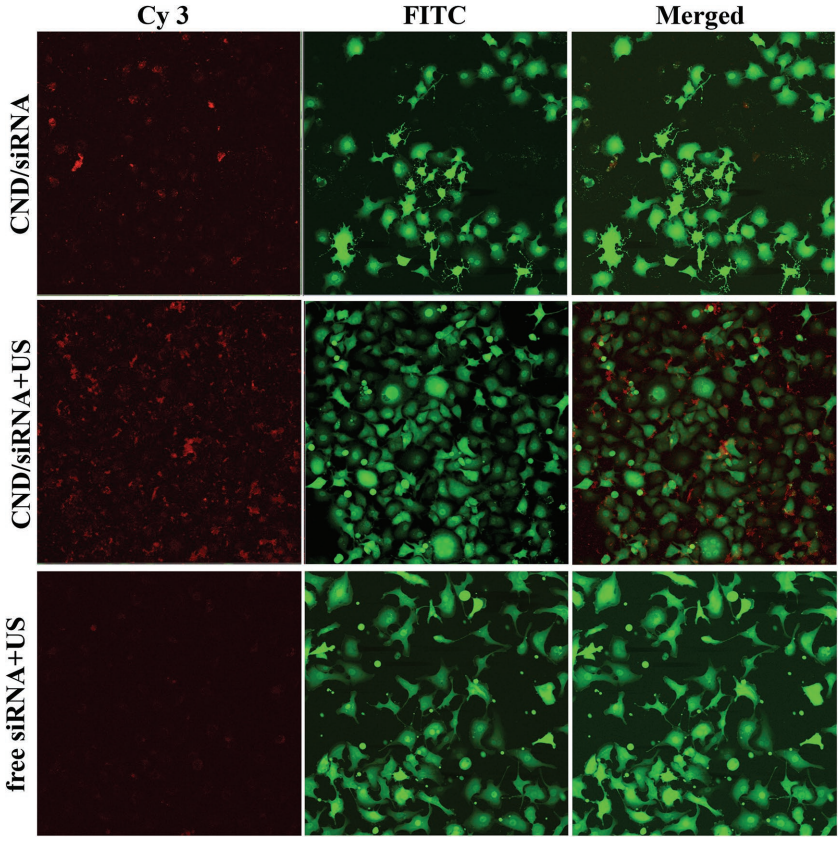

Figure 5. Confocal microscope images of the Cy3-labeled siRNA using CND/siRNA complex or free siRNA with MCF 7 cells expressing GFP after 5 min of incubation. One of the cell chambers treated with CND/siRNA complexes was exposed to ultrasound after incubation (500 kHz, 1 MPa peak-to-peak focal pressure, 40 cycles per burst, 1 kHz PRF, 10 s duration). The last column shows merged images from first and second columns.

3. Conclusion

The aim of this study was to investigate particle stabilized liquid nanodroplets as a vehicle for ultrasound mediated delivery of siRNA. Complexes consisting of chitosan-deoxycholic acid nanoparticles containing perfluoropentane and iron oxide were successfully prepared and conjugated to cell death control siRNA. The complexes were found to be stable at 37 °C for up to 4 h in serum (Figure S4, Supporting Information). Breast cancer cells and lung cancer cells were exposed to ultrasound (500 kHz, 1 MPa peak-to-peak focal pressure, 40 cycles per burst, 1 kHz pulse repetition frequency, 10 s duration) in the presence of the complexes or similar particles that did not contain PFP. We verified that the functionality of siRNA was not adversely affected by the treatment protocol and identified the optimal ratio of siRNA to nanodroplets. We also confirmed the potential for magnetic localization of the complexes using an externally applied magnetic field. Both delivery and gene silencing were successfully demonstrated, with a fourfold reduction in cell viability being produced by the CND-siRNA complexes compared to the control group. Monitoring of acoustic emissions throughout the ultrasound exposure period indicated that there was a positive correlation between the energy of these emissions and treatment efficacy.

4. Experimental Section

Materials: Deoxycholic acid, chitosan oligosacharide, N-hydroxysuccinimide (NHS), heparin sodium salt from porcine intestinal mucosa (heparin), dimethyl sulfoxide (DMSO), gel-loading buffer, and tris-borate-EDTA (TBE) buffer were purchased from Sigma-Aldrich (Dorset, UK). AllStars HS cell death control siRNA and scrambled siRNA was ordered from Qiagen (Manchester, UK). Perfluoropentane (99%) was obtained from Apollo Scientific (Cheshire, UK). Silencer GFP siRNA, Lipofectamine 2000, fetal bovine serum (FBS), PBS, and Dulbecco's modified Eagle's medium (DMEM) were obtained from Life Technologies Ltd (Paisley, UK). Annexin V-FITC, PI, and nuclease-free water was purchased from ThermoFisher Scientific (Bicester, UK). Iron oxide (Fe_2O_3) nanoparticles coated with oleic acid were synthesized using capillary microfluidic devices (d_0 = 7.5 ± 0.35 nm, C_{Fe} = 0.48 mol L^{-1}) as described in previous work.[21] All chemicals were of reagent grade and used without further purification.

Nanoparticle Fabrication: In order to enable siRNA attachment to the nanodroplet surface, it was necessary to modify the formulation from that previously published.[9] Amphiphilic chitosan oligosaccharide and deoxycolic acid (COSD) were synthesized by a coupling reaction of succinimido deoxycholic acids to the primary amine group of chitosan chains[22] (Figure S1, Supporting Information). COSD nanoparticles (CPs) incorporating magnetic nanoparticles in their core were prepared by an oil-in-water emulsification method. COSD nanodroplets (CNDs) were then generated by sonication of CPs in the presence of PFP. Deoxycholic acid is strongly hydrophobic and thus PFP can be stabilized in the particle core. The chitosan amino groups impart a positive charge to both the CPs and CNDs surfaces enabling siRNA to be easily bound through electrostatic interactions (Figure 1a).

Deoxycholic acid (200 mg, 0.5 mmol) and NHS (76 mg, 0.67 mmol) were dissolved in anhydrous tetrahydrofuran (20 mL). Following the addition of 1,3-dicyclohexylcarbodiimide (136 mg, 0.67 mmol), the solution was stirred at 4 °C for 6 h. The urea byproducts were removed by filtration; the filtrate was poured into cold *n*-hexane (120 mL), and then the precipitates were dried in vacuum overnight. The prepared succinimido deoxycholates were reacted with the primary amine groups of chitosan oligosaccharide (COS) via the carbodiimide couple reaction, forming chitosan grafted with deoxycholates (COSD). COS (80 mg) was dissolved in a 9/1 (v/v) mixture of DMSO and deionized water, and then succinimido deoxycholates (49.8 mg) were added to the solution. The reaction mixtures were magnetically stirred for 12 h at room temperature. The resulting solutions were then precipitated into the excess amount of acetone. The precipitates were recovered by centrifugation at 2000 rpm for 5 min, washed with acetone twice and dried under vacuum.

After dispersion of the dried COSD in distilled water, the suspension (5 mg mL^{-1}) was sonicated with an ultrasonic cell disruptor (XL 2000, Misonix Inc. Farmingdale, NY, USA) for 1 min. The prepared suspension was filtered through a 1.0 µm pore syringe filter to remove large aggregates; then 100 µL of the iron oxide nanoparticles in chloroform was added to the filtered suspension. The mixture was sonicated for 30 s and the solvent then evaporated with stirring. The resulting suspension of COSD nanoparticles (CP) was sonicated for a further 10 s with perfluoropentane to prepare COSD nanodroplets.

Nanoparticle Characterization: The hydrodynamic diameters of the prepared CPs and CNDs were measured using a zeta-potential and particle size analyzer (Malvern Instruments, UK) in triplicate at 37 °C. The concentration of nanodroplets dispersed in water was measured by nanoparticle tracking analysis (NanoSight, UK). The size and shape of the particles were determined using bright field TEM (FEI Tecnai 12, USA). 10 µL of each suspension was dispersed in aqueous solution (2 mg mL^{-1}) and deposited on a Formvar/carbon-supported copper grid. The grid was dried in air for 1 h at room temperature and samples were stained with 2% (w/v) of uranyl acetate solution before examination to enable visualization of the polymer.

siRNA Attachment: Cell death control siRNA was used to determine any synergistic effect on the inhibition of cell proliferation with ultrasound. siRNA-CND complexes were prepared with different weight ratios (wr) of CND to siRNA from 3 to 48. siRNA (13 µg, 1 nmol) dissolved in nuclease-free water was mixed with CND (wr 39, 78, 156, 312, and 624) diluted with nuclease-free water. The mixture was incubated at room temperature for 20 min. The apparent zeta potential of both CND and siRNA-CND complexes was measured using the same zeta-potential and particle size analyzer (Malvern Instruments, UK) at 20 °C. To confirm binding of siRNA to the CND, electrophoresis (1% agarose gel) was carried out at 110 V for 15 min in TBE buffer. The band was stained with ethidium bromide (EtBr) included in the agarose gel.

Acoustic Response: A multilayered acoustic resonator with an optically transparent chamber was used to compare the performance of different nanodroplet formulations, in terms of their phase transition efficiency and drug release upon exposure to ultrasound. Details of this device have been published previously[9] but briefly the resonator consists of a piezoelectric transducer, a carrier layer which couples the acoustic energy to the other components of the device, a fluid layer with nanodroplets in suspension, and a reflector layer which reflects the acoustic energy back into the device. The experimentally measured resonance frequency for the device was ≈1.85 MHz, in agreement with computational predictions. The transducer was driven with a continuous wave at a fixed peak-to-peak voltage of 40 V. The resulting peak rarefactional pressure in the chamber was 335 kPa, measured with a calibrated fiber optic hydrophone (Precision Acoustics, Dorchester, UK). To observe the response of CNDs to ultrasound 400 µL of the prepared suspension was pipetted into the device and covered using a glass slide. The device was then mounted on the stage of Nikon TI Eclipse fluorescent microscope (Nikon UK Ltd, Kingston upon Thames, UK) and the solution exposed to ultrasound for the period of interest (between 0 and 90 s) at room temperature.

Magnetic Response: To observe magnetically guided accumulation and in situ vaporization, a cubic neodymium cross-section permanent magnet (NdFeB, N52, 12 mm x 12 mm × 12 mm, CMS Magnetics) and piezoelectric transducer (14 mm × 15 mm × 2 mm, PZ26, Meggit PLC, UK) were assembled in a microfluidic device comprising of a 127 µm × 50 µm (width × thickness) straight microchannel. The microchannel was fabricated using a replica molding microfabrication technique.[16] The CND suspension was flown through the channel at a flow rate 0.2 mL h^{-1} controlled using a syringe pump (NE-1000 New Era Pump Systems, Inc, Hertfordshire, UK). Continuous wave ultrasound was applied during the flow (1.85 MHz, peak rarefactional pressure of 335 kPa, peak-to-peak voltage of 40 V). Accumulation and vaporization of nanodroplets were observed under an optical microscope. Images were acquired with a Nikon Eclipse Ti microscope (Nikon Instruments Europe B.V., Amsterdam, The Netherlands).

siRNA Viability: Free siRNA in DEPC aqueous suspension was exposed to ultrasound using the device described above for periods ranging from 0 to 120 s (1.85 MHz, peak rarefactional pressure of 335 kPa, peak-to-peak voltage of 40 V). Electrophoresis (1% agarose gel) was then carried out at 110 V for 15 min in TBE buffer to determine whether or not the siRNA had been structurally damaged. The band was stained with EtBr included in the agarose gel. The viability of A549 cells (human lung cancer cells) was also evaluated to determine whether the gene silencing activity of the siRNA had been affected by ultrasound exposure. A549 cells were seeded at a 96-well plate at a density of 1×10^4 cells per well and grown in DMEM supplemented with 10% FBS at 37 °C for 24 h. The culture medium was replaced with DMEM containing 20×10^{-9} M siRNA-lipofectamine complexes, and further incubated for 48 or 72 h at 37 °C. The number of viable cells was determined using the MTS colorimetric assay (Promega UK, Southampton, UK). Next, CND–siRNA complexes were exposed to ultrasound with the same conditions for 0, 30, 60, and 180 s and subjected to gel electrophoresis to assess release of siRNA.

Cell Viability: The cytotoxicity of the nanoparticles and nanodroplets was evaluated by examining the inhibition of cancer cell proliferation. The relevant suspensions were diluted with PBS to give a final concentration of siRNA of 20×10^{-9} M (where relevant) based on the binding efficiency determined via electrophoresis as above and the relative concentrations of siRNA and CND/CP in the suspension. A549 cells were seeded in Ibidi cell dishes at a density of 1×10^5 cells per dish and grown in DMEM at 37 °C for 24 h. The culture medium was replaced with serum-free DMEM containing one of the following: (i) CND with cell death control siRNA (CND/siRNA), (ii) CND/GFP siRNA (CND/neg), and (iii) nanoparticles with cell death control siRNA (CP/siRNA). The cell culture dishes were sealed using acoustically compatible polydimethylsiloxane (PDMS) lids.[23] Devices were mounted on top of a permanent magnet Halbach array.[24] The cells were incubated at 37 °C for 5 min before treatment.

For ultrasound exposure, the assembly was aligned with the focus of a 500 kHz single-element focused ultrasound transducer (model H-107B-10; Sonic Concepts, USA) in a tank containing degassed, deionized water at 37 °C. The transducer featured a rectangular cutout through which an imaging linear array (model L11-4v; Verasonics Inc., USA) was aligned.[25] Samples were exposed to 10 s of ultrasound (pulse center frequency of 500 kHz, 1 MPa peak-to-peak focal pressure, 40 cycles per burst, 1 kHz pulse repetition frequency[26]) at five points 3 mm apart, while the imaging array passively recorded the acoustic

emissions from every 10th burst for the first second of each exposure (100 frames, 128 channels, 170 µs per run) to an ultrasound research platform (Verasonics V1; Verasonics Inc., USA) for subsequent analysis.

After ultrasound exposure, cells were further incubated at 37 °C for 24 h. The number of viable cells was determined using the MTS colorimetric assay. To assess apoptosis, treated A549 cells were stained with annexin V-FITC and PI solution. The cells were collected by centrifuging at 1100 rpm for 5 min after treatment and washed twice in PBS. Washed cells were suspended in a binding buffer and then annexin V-FITC and PI solution were added. The cell solution was gently vortexed and incubated for 15 min at room temperature in the dark. The fluorescence intensities of annexin V-FITC and PI were analyzed by flow cytometry (FACSort, BD Bioscience, Oxford, UK). Cell populations containing annexin V-FITC and PI were analyzed to determine the numbers of early/late apoptotic and dead cells.

MCF-7 cells (human breast cancer cells) expressing GFP were seeded in Ibidi cell dishes at a density of 5×10^4 cells per dish and incubated for 24 h with DMEM supplemented with 10% FBS. Cy3 labeled siRNA-CND complexes was prepared to compare the level of cellular uptake promoted by different ultrasound exposure conditions. The culture medium was replaced with Opti-MEM to which were added either CND-siRNA complexes or free siRNA of 10×10^{-9} M. The cell culture dishes were then sealed using PDMS lids, mounted on top of a permanent magnet Halbach array and exposed to ultrasound as described above. After treatment with one of the siRNA formulations and/or ultrasound, cells were washed with PBS three times and fixed with 4% formaldehyde solution in PBS. The cells were then observed in the Ibidi chamber by confocal microscopy (Zeiss780, Zeiss, Cambridge, UK). Images were collected using 488 and 561 nm laser lines for excitation and a 20× objective.

Cavitation Monitoring: The acoustic emissions captured by the imaging array for each experiment were high-pass filtered at 1 MHz to remove the main drive signal and mapped in space to provide an estimate of the acoustic power of cavitation emissions using the reconstruction algorithm described in ref. [27] Acoustic maps over a 20×20 mm area about the ultrasound focus were generated for each frame of the received data. The sum of these maps from each experiment was used to estimate the total energy of acoustic emissions, and overlaid on pre-exposure B-mode images to indicate their spatial distribution. In addition, the maximum value in the maps for each individual frame was used to evaluate the evolution of cavitation activity over time.

Supporting Information

Supporting Information is available from the Wiley Online Library or from the author (doi.10.5287/bodleian:QyZaRYqA1).

Acknowledgements

The authors would like to thank James Fisk and David Salisbury for construction of the transducer and phantom holders used in this study. Calum Crake acknowledges the support of the RCUK Digital Economy Programme Grant No. EP/G036861/1 (Oxford Centre for Doctoral Training in Healthcare Innovation). In addition, the authors are grateful to the EPSRC for supporting this research through Grant No. EP/I021795/1 and Programme Grant No. EP/L024012/1 (OxCD3: Oxford Centre for Drug Delivery Devices).

Received: November 6, 2016
Revised: January 7, 2017
Published online: February 13, 2017

[1] D. Cheng, N. Cao, J. Chen, X. Yu, X. Shuai, *Biomaterials* **2012**, *33*, 1170.
[2] M. Stevenson, V. Ramos-Perez, S. Singh, M. Soliman, J. A. Preece, S. S. Briggs, M. L. Read, L. W. Seymour, *J. Controlled Release* **2008**, *130*, 46.
[3] a) A. I. Minchinton, I. F. Tannock, *Nat. Rev. Cancer* **2006**, *6*, 583; b) K. M. Laginha, S. Verwoert, G. J. Charrois, T. M. Allen, *Clin. Cancer Res.* **2005**, *11*, 6944.
[4] A. R. Carson, C. F. McTiernan, L. Lavery, M. Grata, X. Leng, J. Wang, X. Chen, F. S. Villanueva, *Cancer Res.* **2012**, *72*, 6191.
[5] a) R. Suzuki, Y. Oda, N. Utoguchi, K. Maruyama, *J. Controlled Release* **2011**, *149*, 36; b) R. E. Vandenbroucke, I. Lentacker, J. Demeester, S. C. De Smedt, N. N. Sanders, *J. Controlled Release* **2008**, *126*, 265.
[6] S. Florinas, J. Kim, K. Nam, M. M. Janat-Amsbury, S. W. Kim, *J. Controlled Release* **2014**, *183*, 1.
[7] a) L. Mullin, R. Gessner, J. Kwan, M. Kaya, M. A. Borden, P. A. Dayton, *Contrast Media Mol. Imaging* **2011**, *6*, 126; b) J. E. Chomas, P. Dayton, D. May, K. Ferrara, *J. Biomed. Opt.* **2001**, *6*, 141.
[8] a) A. Mahapatro, D. K. Singh, *J. Nanobiotechnol.* **2011**, *9*, 55; b) B. R. Smith, P. Kempen, D. Bouley, A. Xu, Z. Liu, N. Melosh, H. Dai, R. Sinclair, S. S. Gambhir, *Nano Lett.* **2012**, *12*, 3369; c) R. K. Jain, T. Stylianopoulos, *Nat. Rev. Clin. Oncol.* **2010**, *7*, 653.
[9] J. Y. Lee, D. Carugo, C. Crake, J. Owen, M. de Saint Victor, A. Seth, C. Coussios, E. Stride, *Adv. Mater.* **2015**, *27*, 5484.
[10] A. A. Doinikov, P. S. Sheeran, A. Bouakaz, P. A. Dayton, *Med. Phys.* **2014**, *41*, 102901.
[11] H. Shen, T. Sun, M. Ferrari, *Cancer Gene Ther.* **2012**, *19*, 367.
[12] S. S. H. S. Min, T. W. Lee, H. Koo, H. Y. Yoon, J. H. Na, Y. Choi, J. H. Park, J. Lee, M. H. Han, R. W. Park, I. S. Kim, S. Y. Jeong, K. Rhee, S. H. Kim, I. C. Kwon, K. Kim, *Adv. Funct. Mater.* **2013**, *23*, 5518.
[13] T. G. Leighton, *The Acoustic Bubble*, Academic Press, London, UK, **1994**.
[14] P. S. Sheeran, V. P. Wong, S. Luois, R. J. McFarland, W. D. Ross, S. Feingold, T. O. Matsunaga, P. A. Dayton, *Ultrasound Med. Biol.* **2011**, *37*, 1518.
[15] D. Bardin, T. D. Martz, P. S. Sheeran, R. Shih, P. A. Dayton, A. P. Lee, *Lab Chip* **2011**, *11*, 3990.
[16] D. Carugo, J. Y. Lee, A. Pora, R. J. Browning, L. Capretto, C. Nastruzzi, E. Stride, *Biomed. Microdevices* **2016**, *18*, 4.
[17] H. Baigude, T. M. Rana, *ChemBioChem* **2009**, *10*, 2449.
[18] J. Wang, Z. Lu, M. G. Wientjes, J. L. Au, *AAPS J.* **2010**, *12*, 492.
[19] a) K. W. Ferrara, *Adv. Drug Delivery Rev.* **2008**, *60*, 1097; b) C. K. Holland, D. D. McPherson, *IEEE Int. Symp. Biomed. Imaging* **2009**, *2009*, 755.
[20] S. E. Logue, M. Elgendy, S. J. Martin, *Nat. Protoc.* **2009**, *4*, 1383.
[21] A. Seth, G. Bealle, E. Santanach-Carreras, A. Abou-Hassan, C. Menager, *Adv. Mater.* **2012**, *24*, 3544.
[22] J. Y. Lee, S. H. Lee, M. H. Oh, J. S. Kim, T. G. Park, Y. S. Nam, *J. Controlled Release* **2012**, *162*, 407.
[23] a) D. Carugo, J. Owen, C. Crake, J. Y. Lee, E. Stride, *Ultrasound Med. Biol.* **2015**, *41*, 1927; b) J. Y. Lee, D. Carugo, C. Crake, J. Owen, M. de Saint Victor, A. Seth, C. Coussios, E. Stride, *Adv. Mater.* **2015**, *27*, 5484.
[24] J. Owen, B. Zhou, P. Rademeyer, M.-X. Tang, Q. Pankhurst, R. Eckersley, E. Stride, *Theranostics* **2012**, *2*, 1127.
[25] C. Crake, M. S. Victor, J. Owen, C. Coviello, J. Collin, C. C. Coussios, E. Stride, *Phys. Med. Biol.* **2015**, *60*, 785.
[26] E. Stride, C. Porter, A. G. Prieto, Q. Pankhurst, *Ultrasound Med. Biol.* **2009**, *35*, 861.
[27] M. Gyöngy, C.-C. Coussios, *J. Acoust. Soc. Am.* **2010**, *128*, EL175.

